

FR760797

PRODUCTION AND DECAY OF THE ( $\pi^+ \pi^- \pi^+$ ) SYSTEM IN THE  
REACTION  $\pi^- d \rightarrow \pi^+ \pi^- \pi^+$  AT 9 GeV/c

-----

M. BAUBILLIER, M. RIVOAL, M.C. TOUBOUL  
L.P.N.H.E. - Université Pierre et Marie Curie - PARIS 6e  
Laboratoire associé à l'IN2P3- FRANCE.

N. ANGENISE, M.T. FOGLI-MUCIACCIÀ, V. PICCIARELLI  
INFN - Istituto di Fisica dell'Università di Bari (ITALY)

Production and decay of the ( $\bar{\eta} \eta \pi^+$ ) system in the  
reaction  $\bar{\pi}^- d \rightarrow d \bar{\eta} \eta \pi^+$  at 9 GeV/c

M. Baubillier, M. Rivoal, M.C. Touboul  
L.P.N.H.E. - Université Pierre et Marie Curie-PARIS  
Laboratoire associé à l'IN2P3-FRANCE.

and

N. Armenise, M.T. Fogli-Muciaccia, V. Picciarelli  
INFN - Istituto di Fisica dell'Università di Bari (Italia)

---

Abstract - In this paper we present a study of the reaction  $\bar{\pi}^- d \rightarrow \bar{\eta} \eta \pi^+ d$  at 9 GeV/c. The mass spectra are in fair agreement with the predictions of a Reggeized pion Deck Model. However, the s channel azimuthal angular distribution indicates a  $\rho$  exchange Deck contribution. The results of the partial wave analysis of the ( $\bar{\eta} \eta$ )<sup>-</sup> system are compared with those obtained in a hydrogen target: the  $J^P=2^+$  contribution is very small (1.5  $\pm$  1.2)% in our data, which are dominated by  $J^P=1^+$  for low mass whereas the  $J^P=0^-, 1^+, 2^-$  have comparable importance in the higher mass region.

## 1) Introduction

The purpose of this paper is to present the main features of the coherent production of the  $(3\pi)^-$  system in the reaction



at 9 GeV/c.

In section 2 we discuss the event selection and the differential and total cross sections. The mass spectra are presented in section 3 and compared with the predictions of a Reggeized pion exchange Deck model. A general agreement is found, but the decay of the  $(3\pi)^-$  system shows clearly that it cannot be the only  $t$ -channel exchange mode. The variation of the slope  $b$  of the four momentum transfer distribution  $t_{dd}'$  as a function of the  $(\pi^0\pi^-)$  mass is studied. Finally, in section 4, we report on the results of partial wave analysis of the  $(3\pi)^-$  system which has been performed by using the Illinois program. The conclusions of the present analysis are discussed in sect 5.

## 2) Data analysis and cross-section.

### 2.1 Summary of the analysis.

We have used 240,000 pictures from the CERN 2m DBC exposed to an R.F. separated beam. The films were treated in two different ways. A first lot of 80,000 pictures was scanned for four prongs with at least one stopping track and for three prongs. This has given 34,000 events which have been measured with the Collège de France Spiral Reader. The rest of the pictures were scanned only for four prongs and measured with manual devices.

### 2.2 Selection of coherent events

The measured events were processed through the CERN chain of programs and only those hypotheses consistent with the observed bubble density were kept.

From 44,000 four prong measurements we obtain 1800 events fitting reaction (1) (4C) with a chi-squared probability bigger than 0.05. The 19,000 three prongs events were fitted treating the unseen deuteron as a missing particle (1C) and using the following cuts on the deuteron range  $R$  projected on the front glass in the chamber system :

$$\begin{aligned} \text{error } \delta R &\leq 1.5 \text{ mm} & (R - \delta R) &\leq 2.5 \text{ mm} \\ \text{and } (R - \delta R) &\leq 4 \text{ mm} & \text{if } |\varphi_d - \varphi_{\text{beam}}| &\leq 15^\circ \end{aligned}$$

These criteria are the same as those applied in similar experiment [1]

Only a small fraction ( $\sim 20\%$ ) of three and four prongs events fitted unambiguously reaction (1). The others were ambiguous, fitting also the (1C) reaction :



In this case, the coherent deuteron events were selected by applying cuts to the neutron-proton effective mass, to the angle between the proton and the neutron and to the recoil momenta in the laboratory reference frame. The cuts were

$$3 \text{ and } 4 \text{ prongs} \quad M(pn) < 1.895 \text{ GeV}$$

$$|\cos \theta_{pn}| > 0.75$$

$$4 \text{ prongs only} \quad 0.35 < \beta = \frac{p_n}{p_p} < 1.05$$

Finally we end up with 1364 four prongs and 291 three prongs events corresponding to the coherent production (1).

### 2.3 Differential and total cross sections

Fig 1 shows the  $d\sigma/dt'_d$  distribution. By fitting this distribution in the region  $0.02 < t'_d < 0.1$  ( $\text{GeV}/c$ )<sup>2</sup> with the exponential function  $Ae^{-bt'_d}$  we obtain a slope of  $b=31. \pm 2$ . ( $\text{GeV}/c$ )<sup>-2</sup>. This value is in good agreement with the one obtained with similar fits in previous experiments producing  $(3\pi)^{\pm}$  coherently in  $\pi^{\pm}d$  interactions [2]. Taking into account the loss at small momentum transfer and correcting for the scanning and measuring efficiency we obtain finally a total cross section  $\sigma = 310 \pm 60 \mu\text{b}$ .

## 3) General features of the $d\pi^+\pi^-\pi^-$ final state.

### 3.1 Effective mass spectra

Fig (2-4) show the two body mass distribution. The  $(\pi^+\pi^-)$  mass combination (Fig 2) is dominated by the  $\rho^0$ , but there is an indication for  $f^0$  production as well. No particular structures are observed in the  $(\pi^+\pi^-)$  mass spectrum. A clear indication of  $d^{*0}$  is seen in the low mass ( $d\pi^-$ ) of Fig 3 and a low  $d^{*++}$  production seems to be present in Fig 4. In the  $(3\pi^-)$  mass spectrum of Fig 5 there is beside the well known  $A_1^-$  bump an appreciable contribution of events in the high mass region ( $A_3$  mass region around  $1.640 \text{ GeV}/c$ ). The  $\pi^+\pi^-$  mass distributions for the  $A_1$  and  $A_3$  regions are shown in figure 6. The  $\rho^0$  is dominant in the  $A_1$  mass region and the  $f^0$  is present in the  $A_3$  mass region.

\*  $t'_d = |t'_d - t_{\min}| t_d$  is the four-momentum transfer to the deuteron and  $t_{\min}$  the minimum kinematically allowed by the Chew-Low plot for the given  $(3\pi)^{\pm}$  mass.

### 3.2 Reggeized Deck Model

We compare our results to the prediction of a Reggeized pion exchange model described by the diagram of Fig 7a. The corresponding matrix element, discussed in details in Ref [1], has been used to produce by Monte Carlo method the curves drawn in Fig 2 to 6. The agreement is reasonable, but not completely satisfactory. One possible explanation for this disagreement could be the existence of other exchange mechanisms, for instance the  $\rho$  exchange contribution reported in Fig 7b. This has been suggested by Berger[3] and evidence has already been observed in other diffractive processes[4]. The use of the  $\phi_s$  s-channel azimuthal angle of the  $(3\eta^- \rightarrow \rho^+\eta^-)$  decay in the  $(3\eta^-)$  rest frame, is very promising in this respect. For a fixed set of the kinematical variables ( $\hat{s}$ ,  $\hat{s}_{qd}$ ,  $t_d$  and  $\hat{\phi}_s$  in our case) the  $\hat{\phi}_s = 0$  region correspond to an interaction dominated by the  $\eta$ -exchange (small  $t_d$  in Fig 7a) and the  $|\hat{\phi}_s| = \pi$  region to the one dominated by  $\rho$ -exchange (large  $t_d$  in Fig 7b).

The experimental distribution in Fig 8 has been obtained by selecting events with  $0.69 \leq M(\eta^+\eta^-) \leq 0.99 \text{ GeV}/c^2$  and  $0.02 \leq t_d \leq 0.1 \text{ (GeV}/c^2)$ . The peak near  $\hat{\phi}_s = 0$  is consistent with the presence of an important pion exchange contribution, whereas events with  $\hat{\phi}_s > \frac{\pi}{2}$  suggest a  $\rho$  exchange. Indeed we plotted in Fig 8 the prediction of the pion exchange Deck model normalized to the total number of events. The lack of events in the left hand peak and the excess in the right hand indicates that the pion exchange amplitude does not saturate the channel amplitude and that  $\rho$  exchange may be present.

### 3.3 Four momentum transfer distribution of the reaction $\bar{p}d \rightarrow \bar{p}\pi^-d$

One of the most characteristic features of low mass inelastic diffraction dissociation is the strong dependence of the slope of the  $d\sigma/dt'$  distribution on the mass of the excited cluster.

In order to investigate this phenomenon we have fitted the four momentum distribution  $t'_d$  with the function

$$d\sigma/dt'_d = A e^{-bt'_d}$$

over the range  $0.02 \leq t'_d \leq 0.1 (\text{GeV}/c)^2$ , and for various values of the  $M(\rho\pi)$  system,

There is no visible structure seen either as a dip or a break in the  $t'_d$  distribution (Fig 1); for all values of  $M(\rho\pi)$  the  $t'_d$  distribution is decreasing exponentially. We have reported in Table (1) the values of  $b$  as a function of  $M(\rho\pi)$ .

The lack of statistic does not allow a detailed analysis, nevertheless there is evidence for a variation of the slope. This behaviour is common to other diffractive processes and many interpretations have been suggested. To avoid kinematical effects we have performed the more sophisticated fit proposed in Ref.[6]. The results are reported in Tab.[1]; we obtain compatible results with both methods. A selection on the  $\phi_s$  angle has been also applied to the events to evidence variations in the production dynamics. There is a tendency for the sample with  $\phi_s < \frac{\pi}{2}$  to have higher slope but the large errors do not allow any conclusion (i. e. for  $m(\rho\pi) < 1.8 \text{ GeV}/c^2$  we obtain by using the classical method  $b=30. \pm 2$  ( $\phi_s < \frac{\pi}{2}$ ) and  $b=26. \pm 2.5$  ( $\phi_s > \frac{\pi}{2}$ )).

TABLE 1

$M(\rho\pi)$ GeV/c <sup>2</sup>	Total Classical fit ref(3)	method of ref(7)
0.8 - 1.1	35 $\pm$ 4	36 $\pm$ 6
1.1 - 1.4	28 $\pm$ 4	28 $\pm$ 4
1.4 - 1.8	22 $\pm$ 4	23 $\pm$ 5

\* We have only fitted region for  $m(\rho\pi) < 1.8 \text{ GeV}/c^2$  where there is a real  $\rho^-$  contributions as it comes out from the partial wave analysis (see sect 4).

4) Partial wave analysis of the  $3\pi$  system.

The Illinois partial wave analysis program is used to determine the spin parity structure of the  $3\pi$  system [7]. Our sample of data has been selected by choosing events with  $0.9 \leq M(3\pi) \leq 2.0 \text{ GeV}/c^2$  and  $|t_0^+| < 0.1(\text{GeV}/c)$  and consists of 1419 events.

In this analysis the decay distributions of the  $3\pi$  system, assumed to decay via dipion intermediate state, are fitted to sets of states  $|J^P M \eta\rangle$  where  $J^P$  represents the spin parity and  $M$  the spin projection of the  $3\pi$  system,  $L$  is the relative angular momentum between the dipion and the third pion and  $\eta$  in first approximation can be considered as the naturality of the exchange particle. The following basic set of states with  $M=0$  has been chosen

$0^- S0^+ (\epsilon\pi)$	$0^- P0^+ (\beta\pi)$	$1^+ S0^+ (\beta\pi)$	$1^+ P0^+ (\epsilon\pi)$
$2^- S0^+ (\epsilon^0\pi)$	$2^- P0^+ (\beta\pi)$	$2^- D0^+ (\epsilon\pi)$	

plus an incoherent isotropic background. Some  $M=1$  ( $J^P=2^+$ ) states have also been added.

The s wave  $\eta^+\pi^-$  system,  $\epsilon$ , is parametrized by the CERN Munich phase shift [ $\delta$ ] and the  $\beta$  and  $\epsilon^0$  by single Breit-Wigner functions.

The dominant contributions of the total  $J^P$  states of the  $3\pi$  system are shown in Figure 9, as a function of  $M(3\pi)$ . The  $3\pi$  system seems to be produced entirely in unnatural parity states. The lower mass region  $M(3\pi) < 1.4 \text{ GeV}$  is dominated by the  $J^P = 1^+$  state whereas in the higher mass region the three states  $0^-, 1^+$  and  $2^-$  are of comparable importance with a little more  $2^-$  near the  $A_2$  region.

The behaviour of the various decay modes is shown in Figure 10. Independently of the  $3\pi$  mass, the  $0^-$  state decays mainly in S wave ( $\epsilon\pi$ ). The  $1^+$  states decay mostly in S wave ( $\beta\pi$ ) in the lower region and equally in ( $\beta\pi$ ) and ( $\epsilon\pi$ ) above. Finally for  $2^-$  in the  $A_2$  region the  $\epsilon\pi$  and  $\epsilon^0\pi$  decays are equally present.

The  $2^+$  contribution in the  $A_2^-$  region is only of  $\sim 1.5 \pm 1.2\%$  nevertheless its presence improves significantly the fit.

In addition we have tried other possible states of spin  $1^+$  or  $2^-$  with  $M=1$ . The final results are not significantly changed and the contribution of the above states are always consistent with zero.

These results are compared to those of Ref(9) for  $\bar{u}^-p \rightarrow \bar{p}^+\pi^+\pi^-$  above 11 GeV/c, which are shown as a continuous line on the Figures 9 and 10. The agreement is fairly good.

b) Conclusions

The following conclusions can be drawn from this study :

i) The main characteristics of the studied reaction are similar to those obtained at other energies. The mass distributions are roughly in agreement with a Reggeized pion exchange Deck model.

ii) The contribution from the above model does not seem to saturate the whole channel amplitude. The  $d\sigma/dt_s$  distribution indicates a  $\rho$ -exchange contribution.

iii) A correlation between the mass and the slope of the  $t'$  distribution seems to be present in our data.

iv) The partial wave analysis of the three pion system confirms the dominance of the  $J^P = 1^+$  state at lower mass values, whereas  $J^P = 0^-, 1^+, 2^-$  contributions are present at higher masses.



REFERENCES

1. a) R. Harris - Ph. D. Thesis PUB 22(1975) - University of Washington-Seattle  
b) L.A. Duna et al - Diffractively produced multipion enhancements in  $\pi^+d$  interactions at 15 GeV/c. To be published
2. a) C.P. Horne et al - Phys. Rev. 11, (1975), 966.  
b) D.P. Wilkins - Thesis for master of sciences - Florida state University  
A study of high energy  $\pi^+d$  deuteron experiment.  
FSH HEP 72-8-23.  
c) K. Paler et al - NP, B33, 13 (1971)  
d) D. Harrison et al. Phys. Rev. D5 (1972), 2730.
3. a) E.L. Berger - Developments in the phenomenology of two to three particle reactions. ANL-HEP-PR-75-32.  
b) E.L. Berger - Phys. Rev. 179, (1969), 1567.  
c) E.L. Berger - ANL-HEP-PR-75-06 - A critique of the Reggeized Deck Model.
4. a) P. Bosetti et al. Nucl. Phys. B103 (1976), 189.  
b) J. Biel et al. Phys. Rev. Letters 36 (1976), 504.  
c) J. Biel et al. Phys. Rev. Letters 36 (1976), 507.
5. a) Kittel et al. Nucl. Phys. B30 (1971), 333.  
b) M. Rivoal et al. Nucl. Phys. B87 (1975), 61.  
c) S. Pokorski et al. Nucl. Phys. B19 (1970), 113.
6. H.I. Mattinen and P. Pirila - Phys. Letters 40B (1972), 127.
7. J.D. Hansen et al. Nucl. Phys. B81 (1974), 403.
8. B. Hyams et al. Nucl. Phys. B64 (1973), 134.
9. G. Ascoli et al. Phys. Rev. D9 (1974), 1963.

FIGURE CAPTIONS

1.  $\frac{d\sigma^-}{dt}$  distribution-the crosshatched region corresponds to the three prong contribution. Obviously, the 3 prong events which come from a limited lot of pictures cannot fill totally the hole at low  $t_d'$
  2.  $\pi^+\pi^-$  and  $\pi^-\pi^-$  mass spectra \*
  3.  $\pi^-d$  effective mass spectrum\*
  4.  $\pi^+d$  effective mass spectrum\*
  5.  $\pi^+\pi^-\pi^-$  effective mass spectrum\*
  6.  $\pi^+\pi^-$  mass spectrum in :
    - 1)  $A_1$  region  $0.9 \leq M_{3\pi} \leq 1.3 \text{ GeV}/c^2$
    - 2)  $A_2$  region  $1.5 \leq M_{3\pi} \leq 1.8 \text{ GeV}/c^2$
  7. The pion exchange (a) and  $\rho^*$  exchange (b) Deck graphs for the reaction  $\pi^-d \rightarrow \pi^-\pi^+\pi^-$ . The blobs represent the full elastic scattering amplitudes.
  8. Distribution of the  $\phi_s$  s-Channel azimuthal angle\*, for  $\rho^*$  events and  $0.02 \leq t_d' \leq 0.1 \text{ (GeV}/c^2)^2$ .
  9. Contributions of  $J^P = 0^-, 1^+, 2^-$  and isotropic background states versus  $M_{3\pi}$  mass for events  $0 \leq t_d' \leq 0.1 \text{ (GeV}/c^2)^2$ .  
The solid lines are drawn by hand through experimental points of  $\pi^-p \rightarrow \pi^-\pi^+\pi^-p$  reaction [Ref.9].
  10. Contributions of partial waves  $\{J^P L M\}$  amplitudes versus  $M_{3\pi}$ .  
As in figure 9., solid lines are results from [Ref 9].
- \* N.B. Solid or dashed curves are the predictions of the Reggeized Deck model.

1974

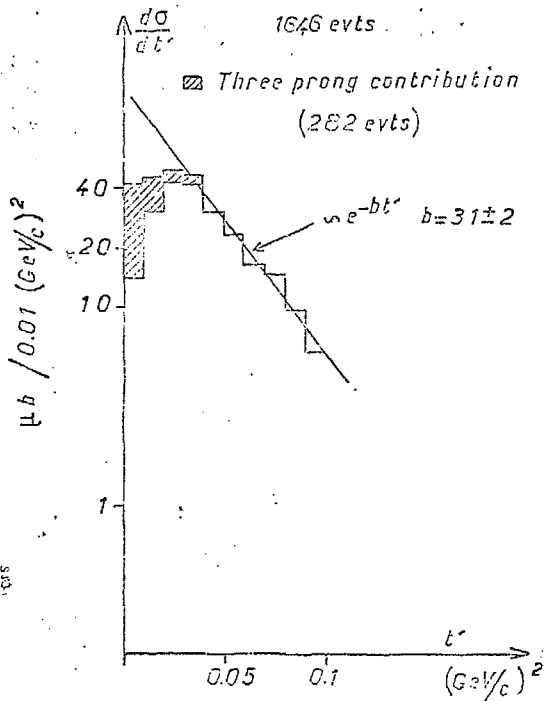


FIG. 1

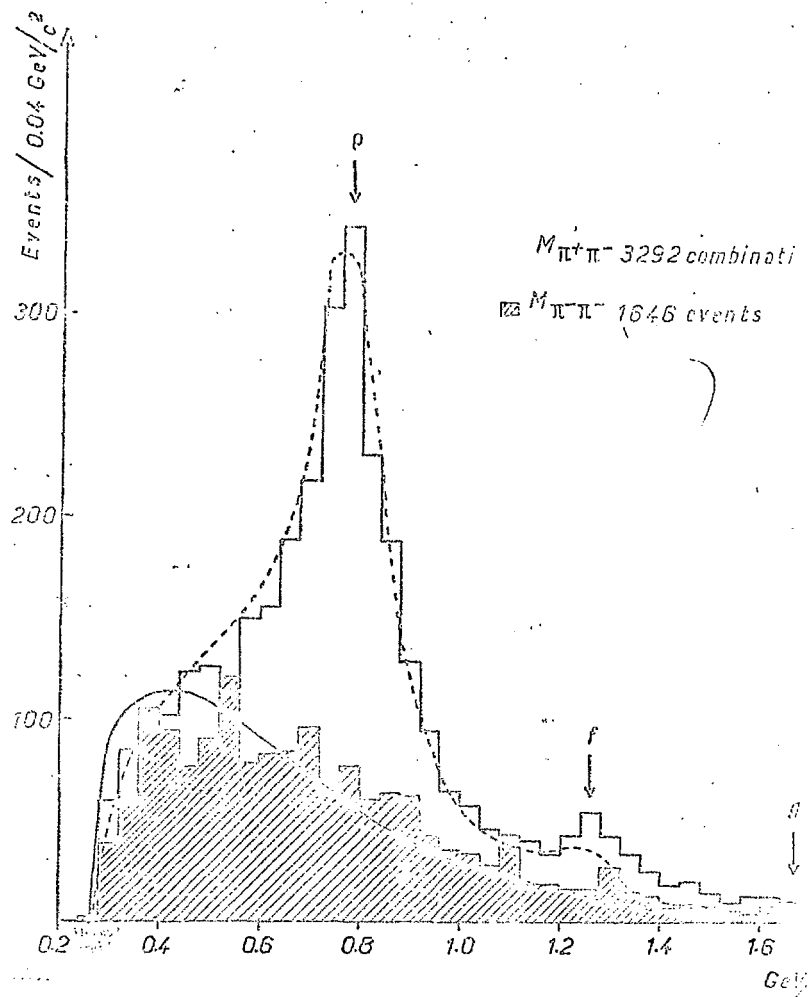


FIG. 2

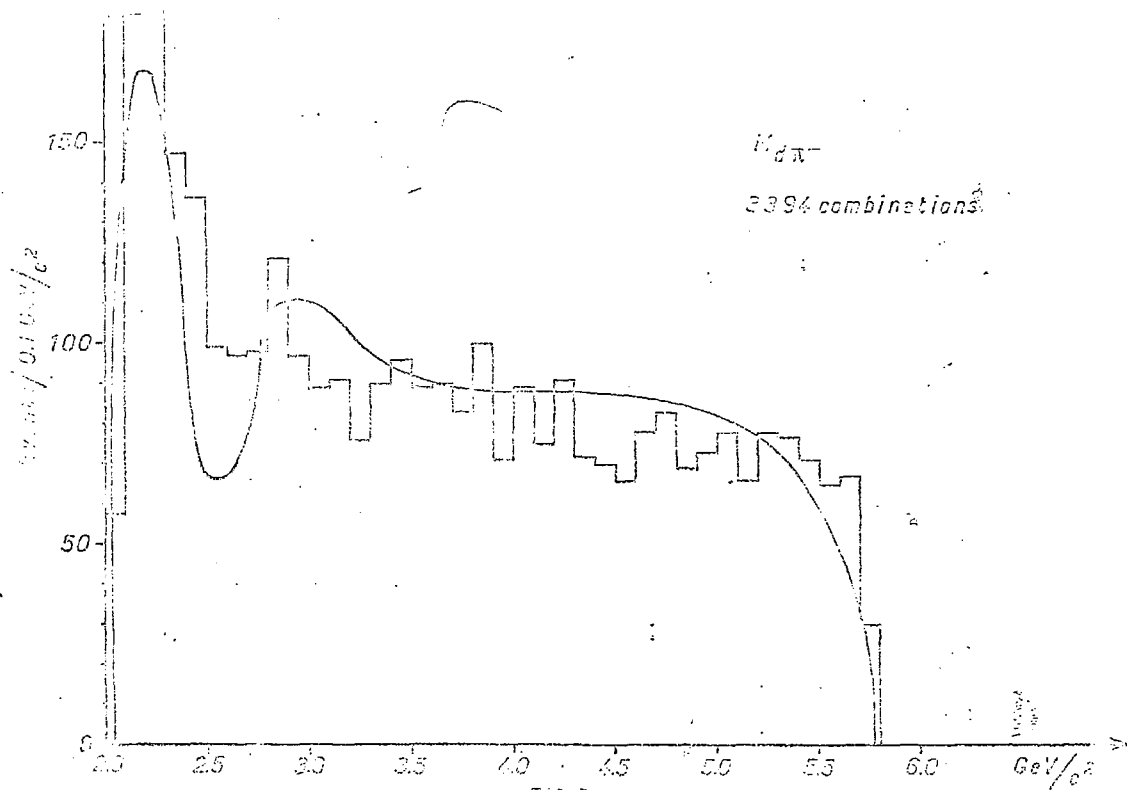


FIG. 3

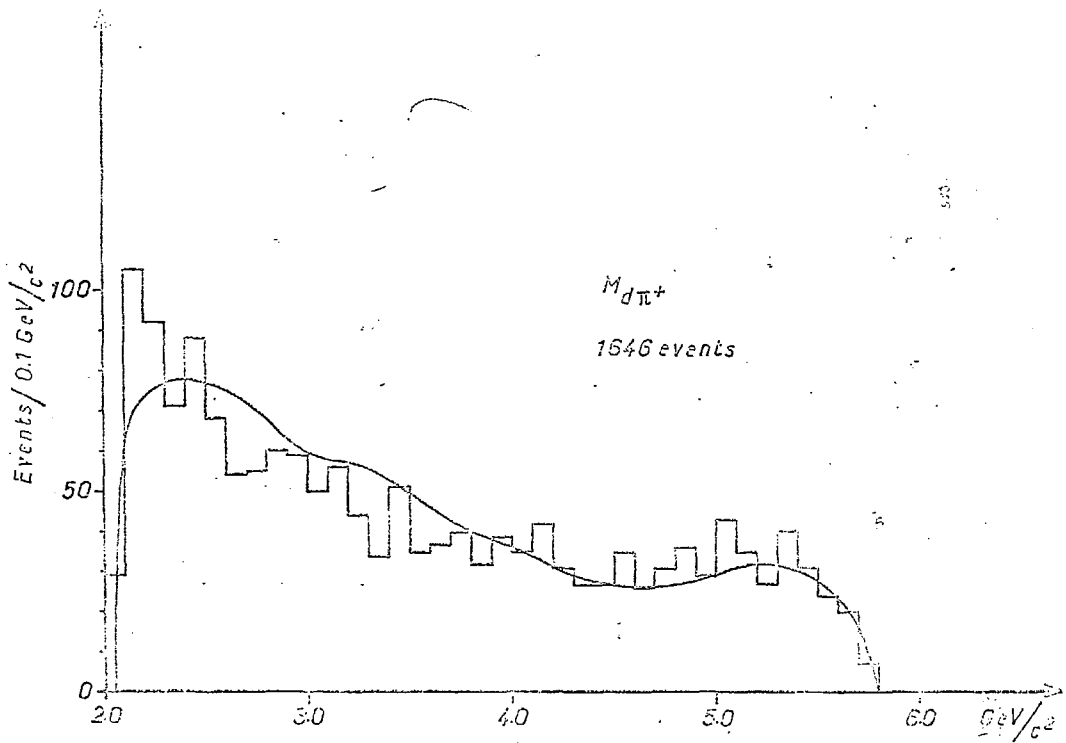


FIG.4

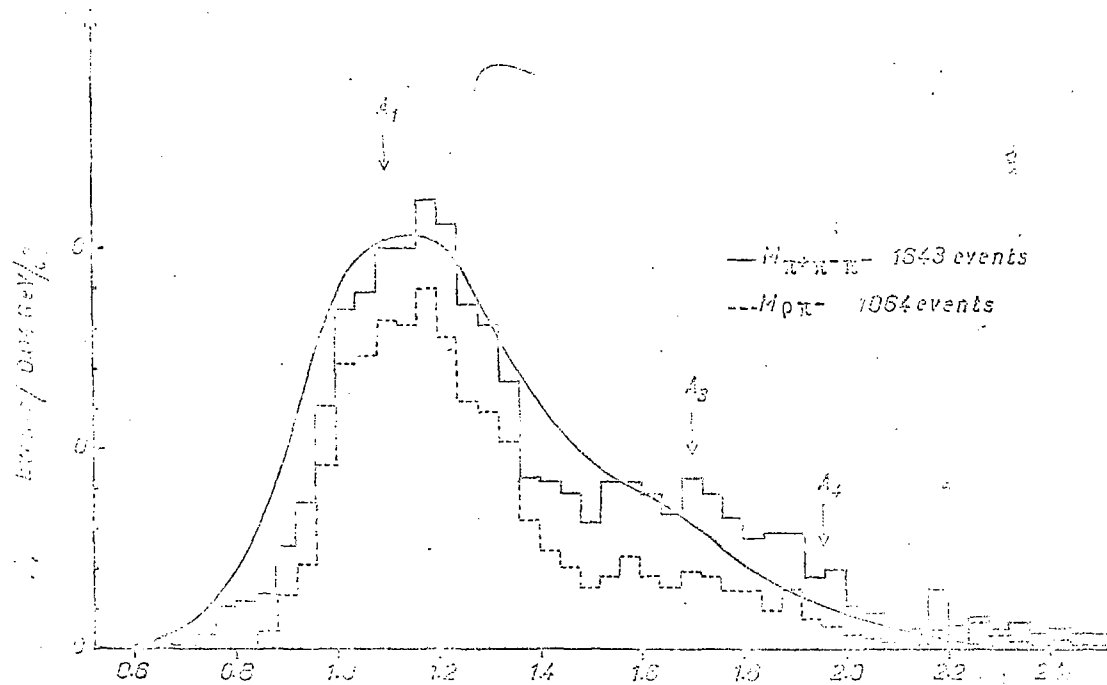


FIG. 5

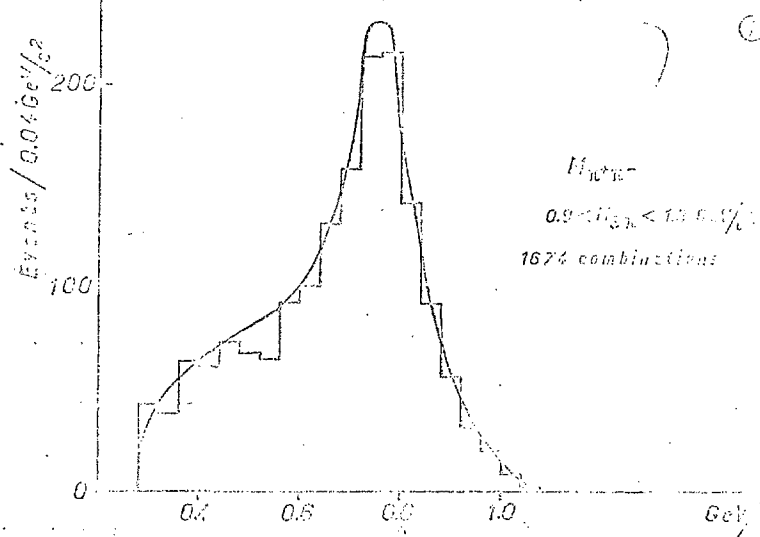
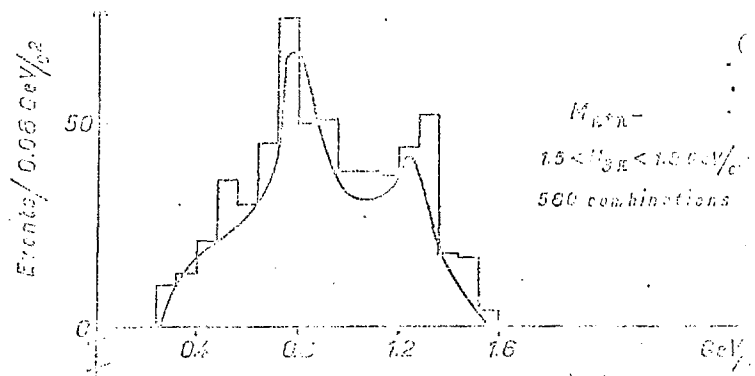


FIG. 6



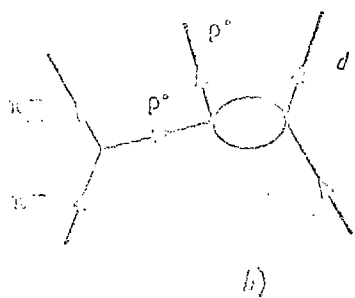
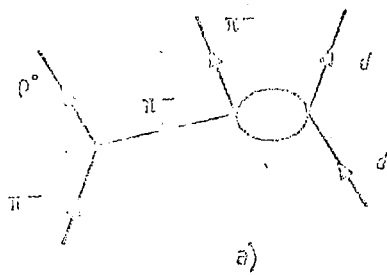
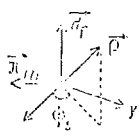
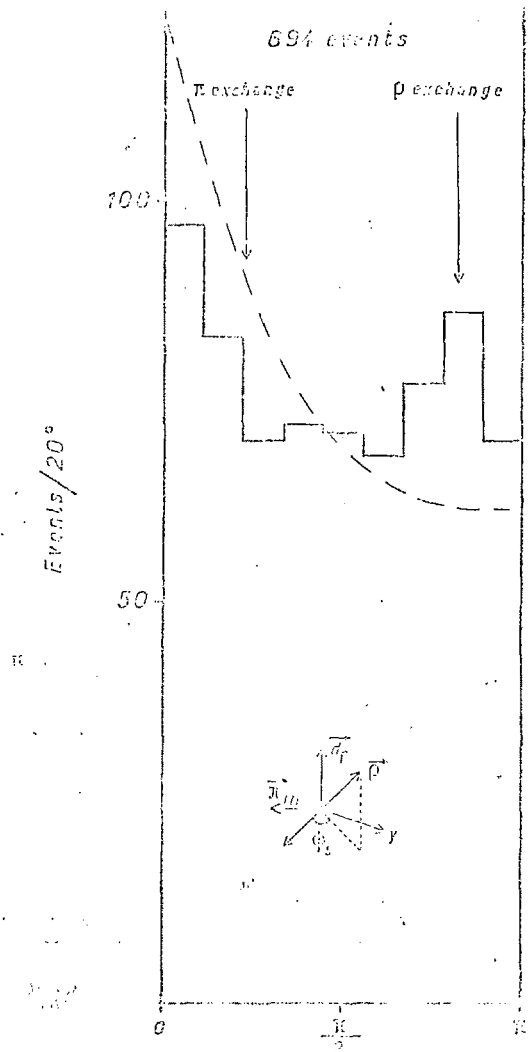


FIG. 7



50

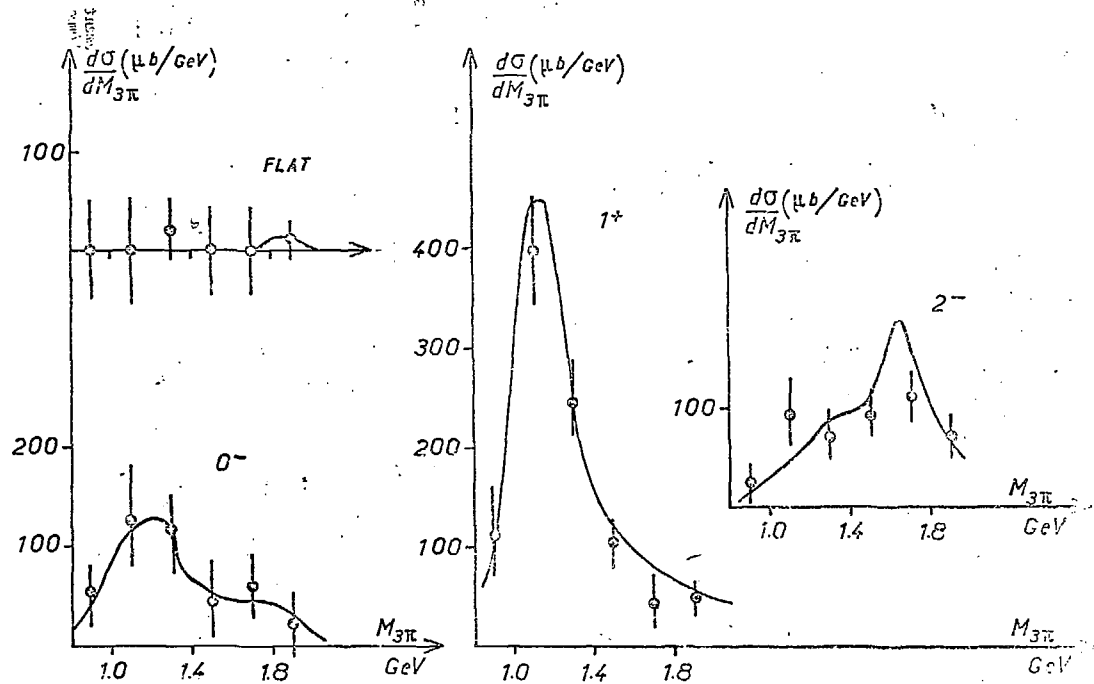


FIG. 9

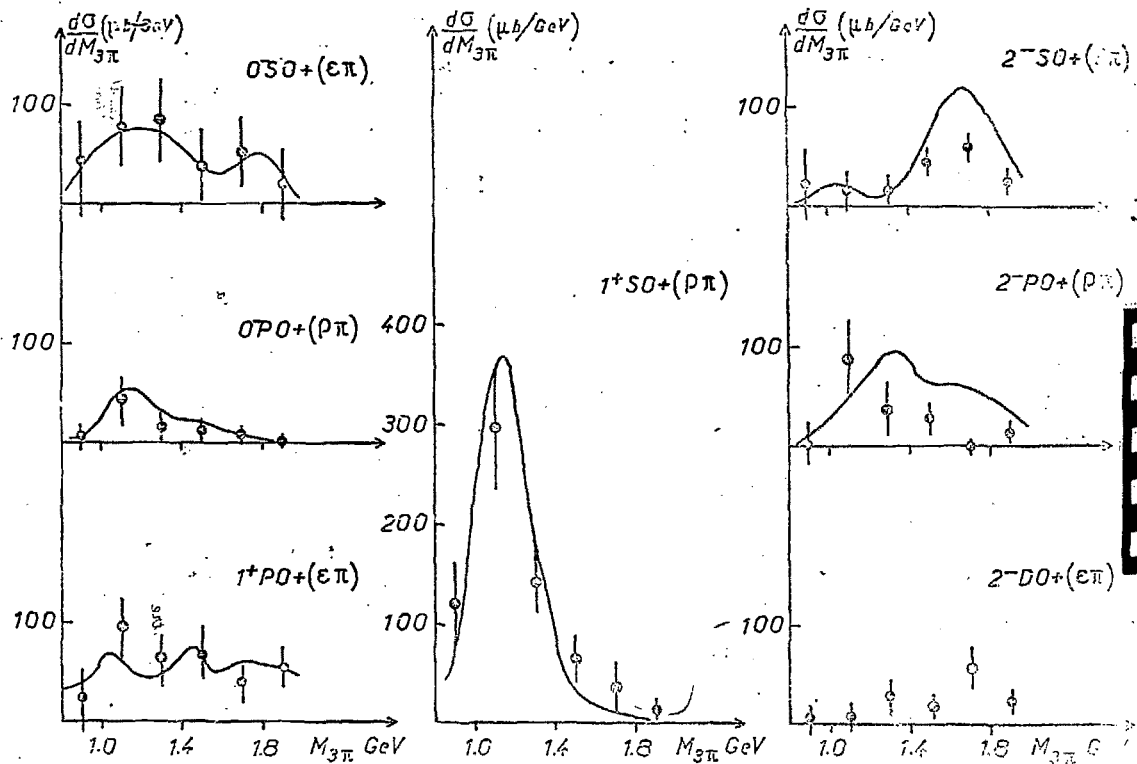


FIG.10